# On the Average Achievable Rate of Spatial Diversity MIMO-FSO over Correlated Gamma-Gamma Fading Channels

Thanh V. Pham *Student Member, IEEE,* Truong C. Thang *Member, IEEE,* and Anh T. Pham *Senior Member, IEEE*

***Abstract*—This paper studies the average achievable rate (AAR) of spatial diversity multiple-input multiple-output (MIMO) free-space optical (FSO) communications over correlated Gamma-Gamma (G-G) fading channels. In particular, we derive the AAR for two different combining techniques at the receiver, namely: equal gain combining (EGC) and maximal ratio combining (MRC). Based on the atmospheric fading correlation analysis and by employing an approximation method for the sum of correlated G-G random variables (RVs), closed-form expressions for AAR are derived for the EGC scheme. For the case of the MRC technique, we first derive the joint probability distribution of correlated G-G RVs with arbitrary correlation coefficient. The AAR is then computed based on the use of the moment generating function (MGF). Numerical results with practical channel correlation coefficients are presented to demonstrate the negative impact of channel correlation on the system performance. Monte-Carlo (M-C) simulations are also performed to validate the analytical results, and an excellent agreement between the analytical and simulation results is confirmed.**

***Index Terms*—FSO, MIMO, correlated Gamma-Gamma fading, average achievable rate.**

## I. Introduction

Free-space optical (FSO) communications has emerged as a promising alternative solution for metro and mobile backhaul networks due to its ability of providing full-duplex, gigabits per second connections [1], [2]. Operating over unlicensed optical frequencies, the technology also effectively addresses the spectrum scarcity problem in radio-frequency (RF) communications. The uncertainty of atmospheric channel, however, poses various challenges in the design of FSO systems. One of the main concerns arises from the presence of atmospheric turbulence, which causes fluctuation in the transmitted optical signal. This fluctuation is known as the turbulence-induced fading or scintillation, which considerably degrades the system performance. Over the years, many techniques have been proposed to alleviate the negative impact of fading, including, remarkably, spatial diversity and multi-hop relaying transmission.

As the turbulence strength is proportional to the link distance, using relay nodes to divide the transmission path into short hops appears to be an obvious solution to reduce the impact of fading [3]–[5]. Though multi-hop transmission technique can significantly improve the link availability, it is not always a cost-effective solution due to the high cost and sometimes infeasibility in construction of FSO relay nodes. In this regard, the use of multiple transmitters and multiple receivers to form a multiple-input multiple-output (MIMO) transmission could be a less complex and more economical solution to combat fading. This technique has also been proven to be effective for improving the reliability of the communication channels by means of spatial diversity [6]–[8]. By introducing additional degrees of freedom in the spatial domain, i.e, transmitting multiple replicas of the same signal over multiple channels and combining them at the receiver, the depth of fading can be substantially reduced [9]. In practical MIMO systems, however, the promising benefit of spatial diversity may not be fully achieved when the fading among sub-channels are correlated, i.e., the separations among transmitters are smaller than the correlation length of the fading. Hence, the impact of channel correlation is crucially important in evaluating the system performance.

Over the past decade, studies on performance analysis of FSO systems have been reported for various channel models [7], [8], [10]–[15]. Of which, the Gamma-Gamma (G-G) turbulence model is mostly assumed due to its accuracy for a wide range of turbulence conditions and tractable mathematical form. For MIMO-FSO systems over correlated G-G channels, there were several studies with the assumption of a simplified channel correlation model, e.g., the exponential correlation model [16], [17]. Nonetheless, the exponential correlation model, which is originally used in RF communications, is not suitable to characterize the correlated atmospheric turbulence channels. Therefore, recent works have been conducted to investigate the characteristics of the atmospheric turbulence-induced fading correlation [18]–[20]. In [18] and [19], by using wave-optics and Monte-Carlo (M-C) simulations, the impacts of turbulence strength, link span, diameter and separation of receiver apertures on the channel correlation have been clarified for receive and transmit diversity systems, respectively. However, since simulation methods can only focus on specific configurations, it is difficult to extend the results to general cases. To deal with this issue, study in [20] has presented the correlation coefficient as a function of the above-mentioned parameters.

Our goal in this paper is to study the average achievable rate (AAR) of spatial diversity MIMO-FSO systems over correlated G-G fading channels with an arbitrary correlation using the analysis in [20]. Regarding the AAR of spatial di-

This work was presented in part at the International Conference on Advanced Technologies for Communications (ATC), Hanoi, Vietnam, Oct. 2016.

Authors are with the Computer Communications Lab., The University of Aizu, Aizuwakamatsu 965-8580, Japan (e-mail: {d8182105 }@u-aizu.ac.jp).

versity MIMO-FSO systems, most of previous studies assumed independent fading channels. The AAR over log-normal fading channels were considered in [21] and [22] with and without bandwidth constraints, respectively. The authors in [23] investigated the AAR for both spatial multiplexing and spatial diversity MIMO-FSO links with pointing error also over log-normal channels. To the best of our knowledge, our study in [7] was the first work on the AAR of spatial diversity MIMO-FSO systems over independent and identically distributed G-G fading. Zhang $et\ al.$ in [8] generalized the results for independent but not necessarily identically distributed fading. In this paper, we aim to extend our previous study by considering correlated G-G fading channels. In particular, the AAR will be computed for two different combining techniques, namely: equal gain combining (EGC) and maximal ratio combining (MRC). To do so, we first utilize an approximation method to the sum of correlated G-G random variables (RVs) proposed in [19] as a benchmark for further analyses. The error behavior of the approximation is also investigated by employing the Kolmogorov-Smirnov (KS) goodness-of-fit test. For the case of EGC, by using the approximation, a closed-form expression in terms of Meijer-G function for the AAR is derived. In the case of MRC, it is more challenging to compute the AAR due to the cumbersome expression of the combined signal. We first derive the joint distribution of correlated G-G RVs with arbitrary correlation matrix. It should be noted that such distribution was studied in [24]. In that work, the G-G fading was considered as arising from multipath fading and shadowing where the shadowing components are generally assumed to be independent. Hence, the correlation coefficient of the G-G fading is a function of the correlation coefficient of the multipath fading only. In the case of atmospheric turbulence channels, the G-G fading arises from large- and small-scale turbulence eddies. As a result, the fading correlation is represented in terms of the correlation coefficients between large- and small-scale turbulence components whose values depend on channel conditions and the structure of receivers. In the conference version of the paper [25], we adopted the joint PDF expression of correlated G-G RVs in [24], which is only valid for the case of independent small-scale turbulence fading, to characterize the atmospheric turbulence channels in FSO systems. The assumption of independent small-scale turbulence fading, however, is not always realistic especially in the case of strong turbulence regime. As a result, a joint PDF expression for the correlated G-G fading (correlated G-G RVs) with arbitrary correlation coefficients of small-scale and large-scale turbulence components should be derived. More explicitly, the main contributions of the paper include

- A closed-form expression for the joint PDF of correlated G-G RVs with arbitrary correlation coefficients of small-scale and large-scale turbulence components. Having the joint distribution of correlated G-G RVs, we then adopt the moment generating function (MGF)-based framework in [26] to calculate the AAR in the case of MRC.
- A proof of the approximation method to the sum of correlated G-G RVs proposed in [19] (Proposition 1) is provided (Appendix A). The error behaviors of the method for different correlation coefficient parameters are thoroughly evaluated through KS goodness-of-fit statistical test.
- Numerical results with realistic link parameters including the turbulence strength and correlation coefficients are comprehensively demonstrated.

The remainder of the paper is organized as follows. In Section II, the G-G fading model and the turbulence channel correlation analysis are described. Section III focuses on an approximation method for the sum of correlated G-G RVs. Based on the method, closed-form expressions for the AAR are derived in Section IV. Section V presents some numerical results and finally we conclude the paper in Section VI.

## II. Gamma-Gamma Turbulence-induced Fading

### A. Gamma-Gamma Model

The G-G model (also known as the Generalized-K model in some studies) has been widely used to characterize the turbulence-induced fading in FSO communications. Let $X$ be a G-G RV which represents the turbulence fading. Originally, $X$ is derived from the product of two independent Gamma RVs, which describe the fading caused by the large-scale and small-scale turbulence components [27]. The probability density function (PDF) of the G-G distribution is given by

$$f_X(x) = \frac{2(\frac{\alpha\beta}{\Omega})^{(\alpha+\beta)/2}}{\Gamma(\alpha)\Gamma(\beta)} x^{(\alpha+\beta)/2-1} K_{\alpha-\beta}\left(2\sqrt{\frac{\alpha\beta x}{\Omega}}\right), \quad (1)$$

where $\Gamma(\cdot)$ is the gamma function, $K_{\alpha-\beta}(\cdot)$ is the modified Bessel function of the second kind and order $\alpha-\beta$ and $\Omega$ is the expected value which, without loss of generality, is normalized to 1. $\alpha$ and $\beta$ are the shaping parameters of the RV which represent the effective numbers of large-scale and small-scale turbulences, and in the case of zero-inner scale they are given by [28]

$$\alpha = \left\{ \exp\left[\frac{0.49\sigma_R^2}{\left(1+1.11\sigma_R^{12/5}\right)^{7/6}}\right] - 1 \right\}^{-1}, \quad (2)$$

$$\beta = \left\{ \exp\left[\frac{0.51\sigma_R^2}{\left(1+0.69\sigma_R^{12/5}\right)^{5/6}}\right] - 1 \right\}^{-1}. \quad (3)$$

The parameter $\sigma_R^2$ denotes the Rytov variance, and for the case of plane wave propagation, it is given by [27]

$$\sigma_R^2 = 1.23 C_n^2 k^{7/6} L^{11/6}, \quad (4)$$

where $k = 2\pi/\lambda$, with $\lambda$ is the optical wavelength, is the optical wave number, $L$ represents the transmission distance and $C_n^2$ is the altitude-dependent index of the refractive structure parameter which determines the turbulence strength. The $n-$th moment of $X$ is given by [29]

$$\mathbb{E}[X^n] = \frac{\Gamma(\alpha+n)\Gamma(\beta+n)}{\Gamma(\alpha)\Gamma(\beta)} \left(\frac{\alpha\beta}{\Omega}\right)^{-n}. \quad (5)$$

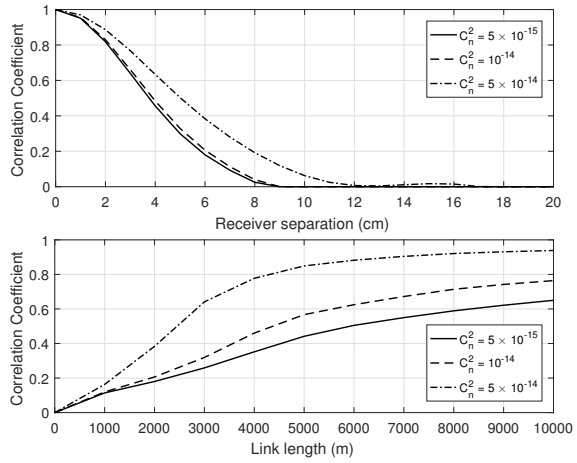


Figure 1: (a) Correlation coefficient versus aperture separation for different values of turbulence strength, link range $L = 2000$ m; (b) Correlation coefficient versus link range for different values of turbulence strength with receiver separation $d = 6$ cm.

### *B. Channel Correlation Analysis*

*1) General Turbulence Conditions:* In practical MIMO-FSO systems, the correlation among sub-channels is sometimes inevitable, especially, for an extended link and/or a relatively small aperture separation. The prediction of the channel correlation is of importance in evaluating the system performance since it significantly affects the spatial diversity gain. In general, the correlation coefficient is a function of the turbulence strength, the link span, the aperture diameter, and the receiver separation. The correlation coefficient $\rho$ between two receivers separated by the distance $d$ is given by

$$\rho = \frac{\omega(d)}{\omega(0)}, \tag{6}$$

where $\omega(d)$ is the spatial covariance function of irradiance, which is given as

$$\omega(d) = \exp\Bigg\{ 8\pi^2 k^2 L \int_0^1 \int_0^\infty \kappa \Phi_{n,\text{eff}}(\kappa) J_0(\kappa d) \times \exp\left(\frac{-D^2\kappa^2}{16}\right)\left[1 - \cos\left(\frac{L\kappa^2\xi}{k}\right)\right] \mathrm{d}\kappa \mathrm{d}\xi \Bigg\} - 1, \tag{7}$$

where $D$ is the receiver aperture diameter, $J_0(\cdot)$ is the Bessel function of the first kind and zero order, and $\Phi_{n,\text{eff}}(\kappa)$ represents the effective atmospheric spectrum [20]. Assume the case of zero-inner scale and infinity-outer scale, $\Phi_{n,\text{eff}}(\kappa)$ can be given by [28]

$$\Phi_{n,\text{eff}}(\kappa) = 0.033 C_n^2 \kappa^{-11/3} \times \left[\exp\left(-\frac{\kappa^2}{\kappa_{X,0}^2}\right) + \frac{\kappa^{11/3}}{(\kappa^2 + \kappa_{Y,0}^2)^{11/6}}\right], \tag{8}$$

with

$$\kappa_{X,0}^2 = \frac{k}{L}\frac{2.61}{1 + 1.11\sigma_R^2}, \tag{9}$$

$$\kappa_{Y,0}^2 = \frac{3k}{L}\left(1 + 0.69\sigma_R^{12/5}\right). \tag{10}$$

An illustration of the relationship between the correlation coefficient and different system parameters is presented in Fig. 1. Generally, the correlation coefficient decreases dramatically when the aperture separation increases and is proportional to the transmission distance. It is also seen that the correlation coefficient increases in accordance with the increase in the refractive structure parameter $C_n^2$. The observation is logical due to the fact that channel correlation between two channels mainly arises from the deflection of optical beams propagating through large-scale turbulence eddies whose sizes are larger than the scattering disk $L/k\rho_0$, where $\rho_0 = \left(1.46 C_n^2 k^2 L\right)^{-3/5}$ is the transverse correlation width (a.k.a spatial coherence scale) [28]. Along the transmission path, these large-scale turbulence eddies can be divided into common eddies where both optical beams go through and independent eddies where either one of the two beams does. The common eddies deflect the two optical beams simultaneously and thus cause channel correlation. When $L$ and/or $C_n^2$ increases, the scattering disk increases as well ($C_n^2$ is inversely proportional to $\rho_0$ thus is proportional to the $L/k\rho_0$), resulting in an increase in the average size of the large-scale turbulence eddies. Accordingly, the probability of having common eddies increases, leading to the higher channel correlation.

*2) Gamma-Gamma (G-G) Turbulence Condition:* In particular to the G-G turbulence model, the correlation $\rho$ can be considered arising partly from large- and small-scale turbulence eddies. As a result, the fading correlation can be represented in terms of the correlation coefficients between large- and small-scale turbulence components. Particularly, given $X_i \sim \Gamma\Gamma(\alpha_i, \beta_i, \Omega_i)$ [1], $X_j \sim \Gamma\Gamma(\alpha_j, \beta_j, \Omega_j)$ and the independence of large- and small-scale, the correlation coefficient between $X_i$ and $X_j$ is given by [27]

$$\rho_{ij} = \rho_{ji} = \frac{\text{Cov}(X_i, X_j)}{\sqrt{\text{Var}(X_i)\text{Var}(X_j)}} = \frac{\rho_{s_{ij}}\sqrt{\alpha_i\alpha_j} + \rho_{l_{ij}}\sqrt{\beta_i\beta_j} + \rho_{s_{ij}}\rho_{l_{ij}}}{\sqrt{\alpha_i + \beta_i + 1}\sqrt{\alpha_j + \beta_j + 1}}, \tag{11}$$

where $\rho_{s_{ij}}$ and $\rho_{l_{ij}}$ are small- and large-scale fading coefficients between $X_i$ and $X_j$, respectively. Cov$(\cdot)$ and Var$(\cdot)$ denote the covariance and the variance operators. Specifically, for the case of identically correlated, i.e., $\rho_{s_{ij}} = \rho_s$ and $\rho_{l_{ij}} = \rho_l$, and identically distributed G-G RVs, i.e., $\alpha_i = \alpha_j = \alpha$, $\beta_i = \beta_j = \beta$, Eq. (11) reduces to

$$\rho = \frac{\alpha\rho_s + \beta\rho_l + \rho_s\rho_l}{\alpha + \beta + 1}. \tag{12}$$

It is seen from the above equation that given a value of $\rho$, there are an infinite number of solutions for $\rho_s$ and $\rho_l$. Therefore, $\rho_s$ and $\rho_l$ should be chosen appropriately to predict

[1]In this paper, we use the notation $X \sim \Gamma\Gamma(\alpha, \beta, \Omega)$ to indicate that the RV $X$ follows the G-G distribution with parameters $(\alpha, \beta, \Omega)$.

the system performance accurately. However, there is a set of criteria for selecting the values of $\rho_s$ and $\rho_l$ depending on the turbulence conditions. In particular, in the *strong turbulence regime*, the intensity fluctuations arising from the small-scale turbulence can be averaged out effectively, leading to $\rho_s \approx 0$. On the other hand, under *weak-to-moderate turbulence regime*, all turbulence eddies of any size affect the propagating beam, which results in $\rho_s = \rho_l$. Finally, under *moderate-to-strong turbulence regime*[2], both small- and large-scale turbulence components affect the multiple apertures simultaneously, while the correlation for the large-scale component is higher than that of the small-scale one. In this case, we can only conclude that $\rho_s < \rho_l$ and the system performance lies between those of the cases when $\rho_s \approx 0$ and $\rho_s = \rho_l$.

## III. Approximation to the Sum of Correlated Gamma-Gamma Random Variables

### A. Approximation Method

In this section, we investigate the distribution of the sum of correlated G-G RVs as the foundation for further performance analyses. Let $\{X_i \sim \Gamma\Gamma(\alpha_i, \beta_i, \Omega_i)\}_1^K$ be a set of $K$ correlated G-G RVs. The sum of them is defined as

$$Z = \sum_{i=1}^{K} X_i. \tag{13}$$

The exact statistic of $Z$, however, remains unknown. Therefore, an approximation approach for the sum of correlated G-G RVs is of great interest due to its simple mathematical form while still providing an acceptable accuracy. For the case of correlated G-G RVs, several approximation methods have been proposed in the literature. In [30], using the moment matching method, the sum of two correlated G-G RVs was approximated by an $\alpha - \mu$ RV. Numerical results showed a good accuracy of the method. However, the parameters of the approximating $\alpha - \mu$ RV can only be obtained numerically using software packages, e.g., MATLAB, due to the difficult nonlinear equations. The use of a Gamma RV as the approximating RV has been studied in [31]. The main drawback of the approach is the need of adjustment parameters, which are introduced to tighten the accuracy in the case of large values of the standard deviation of the summands. In [32], the PDF and the cumulative distribution function (CDF) of the sum of correlated G-G RVs were approximately represented through finite series forms that are cumbersome to use in analyzing the channel achievable rate. Another approach that uses a G-G RV for the approximation has been proposed in [19]. However, expressions for deriving the parameters of the approximating G-G RV had not been clarified. In this paper, we adopt the approach in [19] and provide a proof for it. Furthermore, we quantitatively evaluate the error behavior of the method through Kolmogorov-Smirnov (KS) goodness-of-fit statistical test [33].

[2]For the sake of simplicity, this uncertain case is excluded in this study. It should be noted that the moderate-to-strong turbulence regime, which is defined as $\sigma_R^2$ is slightly larger than 1, does not necessarily include the strong turbulence one which corresponds to $\sigma_R^2$ apparently larger than 1.

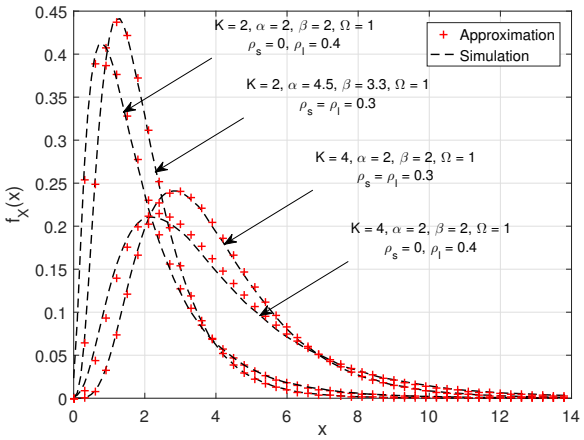


Figure 2: PDF plots of the sum of correlated G-G RVs and the approximating G-G RV.

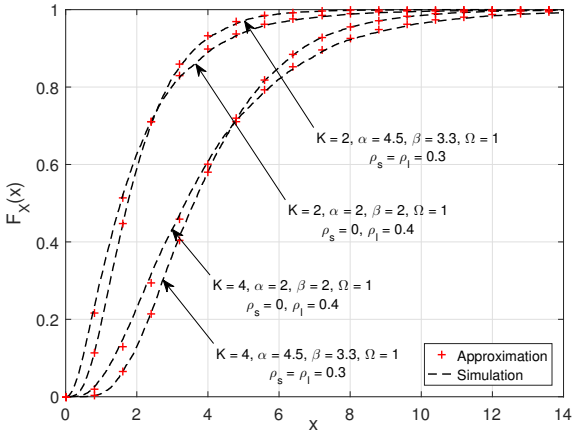


Figure 3: CDF plots of the sum of correlated G-G RVs and the approximating G-G RV.

*Proposition 1:* The sum of $K$ statistically correlated and identically distributed G-G RVs, i.e., $\{X_i \sim \Gamma\Gamma(\alpha, \beta, \Omega)\}_1^K$, can be accurately approximated by another G-G RV, e.g., $Y$ whose parameters $(\overline{\alpha}, \overline{\beta}, \overline{\Omega})$ are given by

$$\overline{\alpha} = h\alpha, \quad \overline{\beta} = h\beta, \quad \overline{\Omega} = K\Omega, \tag{14}$$

where $h$ is given by

$$h = K\left(1 + \frac{2}{K}\sum_{i=1}^{K}\sum_{j=i+1}^{K}\rho_{ij}\right)^{-1}, \tag{15}$$

with $\rho_{ij}$ being the correlation coefficient between $X_i$ and $X_j$.

*Proof:* See appendix A.

### B. Numerical Examples

We demonstrate the accuracy of the approximation method by comparing the statistic of the approximating RV $Y$ with that of the simulation data. The simulated PDF and CDF of the sum of G-G RVs generated from $2 \times 10^6$ samples by Monte-Carlo (M-C) method are used for reference. The generation of $K$ correlated G-G RVs for the simulation is based on generating

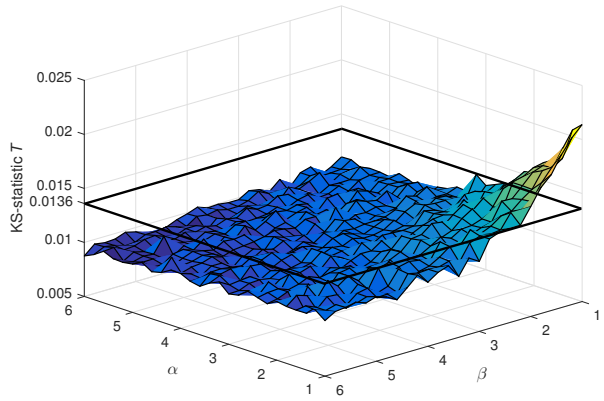


Figure 4: KS goodness-of-fit test for $K = 2$ and $\rho_s = \rho_l = 0.3$.

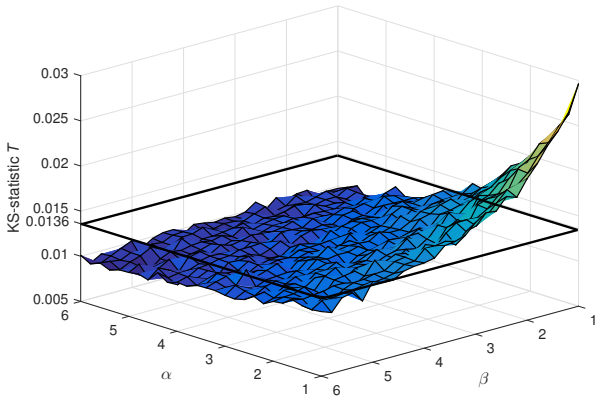


Figure 5: KS goodness-of-fit test for $K = 2$ and $\rho_s = 0$, $\rho_l = 0.4$.

two separate sets of $K$ correlated Gamma RVs. Using the Decomposition Method [34], correlated Gamma RVs with arbitrary correlation coefficient can be generated efficiently.

Firstly, Fig. 2 and Fig. 3 compare the PDFs and CDFs of the approximating G-G RV with that of the simulation data for different shaping parameters ($\alpha$, $\beta$) of the approximated G-G RVs, correlation coefficients and numbers of summands $K$, respectively. Specifically, Table I shows the obtained parameters of the approximating G-G RV for the considered settings.

Table I: Parameters of the approximating G-G RV.

| Approximated G-G RVs, $X_i$ | | Approximating G-G RV, $Y$ |
|---|---|---|
| $K = 2$ | $\alpha = 4.5$, $\beta = 3.3$<br>$\rho_s = \rho_l = 0.3$<br>$\Omega = 1$ | $\overline{\alpha} = 7.0525$<br>$\overline{\beta} = 5.1719$<br>$\overline{\Omega} = 2$ |
| | $\alpha = 2$, $\beta = 2$<br>$\rho_s = 0, \rho_l = 0.4$<br>$\Omega = 1$ | $\overline{\alpha} = 3.4483$<br>$\overline{\beta} = 3.4483$<br>$\overline{\Omega} = 2$ |
| $K = 4$ | $\alpha = 4.5$, $\beta = 3.3$<br>$\rho_s = \rho_l = 0.3$<br>$\Omega = 1$ | $\overline{\alpha} = 9.8446$<br>$\overline{\beta} = 7.2194$<br>$\overline{\Omega} = 4$ |
| | $\alpha = 2$, $\beta = 2$<br>$\rho_s = 0, \rho_j = 0.4$<br>$\Omega = 1$ | $\overline{\alpha} = 5.4054$<br>$\overline{\beta} = 5.4054$<br>$\overline{\Omega} = 4$ |

It is clearly seen that there are always excellent fits between the approximation and the simulation results. To quantitatively evaluate the error behavior of the approximation method, we employ the Kolmogorov-Smirnov (KS) goodness-of-fit statistical test, which measures the maximum value $T$ of the absolute different between the empirical CDF of the sum $Z = \sum_{i=1}^{K} X_i$ and the approximating RV $Y$, i.e.,

$$T \triangleq \left| F_Z(x) - F_Y(x) \right| \tag{16}$$

To verify an approximation, the KS goodness-of-fit test compares the statistical test value $T$ with a critical level $T_{max}$ for a significance level $\phi$. An approximation is said to be accepted with significance level $(1 - \phi)$ if $T \leq T_{max}$, while it is considered to be rejected with the same significance level if $T > T_{max}$. The critical value of $T_{max}$ is given by $T_{max} = \sqrt{-\frac{1}{2v} \ln \frac{\phi}{2}}$ with $\phi$ is the significance level and $v$ is the number of samples of RV for the simulation. Here, we choose the typical values $\phi = 5\%$ and $v = 10^4$, resulting in the critical value $T_{max} = 0.0136$ [35]. In Fig. 4, we show the KS statistic test of the approximation method with $K = 2$, $\rho_s = \rho_l = 0.3$ and $\Omega = 1$ for different values of $\alpha$ and $\beta$. The presented result is obtained by averaging the results of 80 simulation runs. We observed that the approximation method is valid, i.e., $T \leq 0.0136$ when either $\alpha$ or $\beta$ is smaller than 2. On the other hand, the method fails when both $\alpha \leq 2$ and $\beta \leq 2$, i.e., very strong turbulence conditions. Fig. 5 illustrates the KS statistic test for the case when $\rho_s = 0$ and $\rho_l = 0.4$. It is seen that compared to the case of $\rho_l = \rho_s$, the approximation method performs worse, especially when $\alpha$ and $\beta$ are small. In particular, it fails when both $\alpha \leq 4$ and $\beta \leq 4$ and is accepted when at least one of the parameters is larger than 4. We will show later in Section V that with typical setup parameters, the value of $\alpha$ is always larger than 4 thus revealing the validity of the approximation method in characterizing the AAR.

## IV. Average Achievable Rate Analysis

### A. MIMO-FSO Transmission

We consider a MIMO-FSO system which is equipped with $M$ transmitters and $N$ receivers. The commonly used intensity modulation/direction detection (IM/DD) scheme with On-Off Keying (OOK) signaling is assumed. The received signals at the receivers are combined by either equal gain combining (EGC) technique or maximum ratio combing (MRC) technique. In both cases, the received signal at the output of the $n-$th receiver can be written as

$$r_n = \eta P_t x \sum_{m=1}^{M} I_{mn} + z_n, \tag{17}$$

where $P_t$ is the average received optical power, $x \in [0, 1]$ represents the information bits, $\eta$ is the optical-to-electrical

conversion coefficient and $z_n$ is the receiver thermal noise which is modeled as stationary Gaussian random process with zero mean and variance $N_0/2$. $I_{mn}$ denotes the fading gain of the link connecting the $m-$th transmitter and the $n-$th receiver, which is modeled as a G-G RV. The spatial separations among transmitters as well as receivers are much smaller than the link range, hence $I_{mn}$'s can be reasonably assumed to be identically distributed. Without lost of generality, we normalize $\mathbb{E}[I_{mn}] = 1$, i.e., $I_{mn} \sim \Gamma\Gamma(\alpha, \beta, 1)$, to ensure that the fading does not degrade or amplify the average transmitted signal power.

### *B. Average Achievable Rate*

It is well known that the atmospheric turbulence over FSO channels is slow in fading, which is equivalent to communication over channels where there is a nonzero probability that any given transmission rate cannot be supported by the channel. Since the coherence time of the channel is in the order of milliseconds, atmospheric turbulence-induced fading remains constant over a large number of transmitted bits [36], [37]. Without any delay constraints, if the codeword extends over at least several atmospheric coherence times, which allows coding across both deep and shallow fade channel realizations, the fast fading regime can be assumed. With proper coding and interleaving, the AAR can be expressed as an average over many independent fades of the atmospheric channel. The AAR is the expectation with respect to the gains of the instantaneous rate [23], [38]

$$C = B \int_0^\infty \log_2(1+\gamma) f_\gamma(\gamma) \mathrm{d}\gamma, \tag{18}$$

where $\gamma$ denotes the instantaneous SNR of the channel, $f_\gamma(\gamma)$ is the PDF of $\gamma$ and $B$ is the channel bandwidth.

*1) Equal Gain Combining (EGC):* For the EGC scheme, the combined signal $r$ at the destination is given as

$$r = \frac{\eta P x}{MN} \sum_{n=1}^{N} \sum_{m=1}^{M} I_{mn} + z, \tag{19}$$

where $P = MP_t$ is the total received optical power and, without lost of generality, is normalized to unity. The scaling factor $MN$ in Eq. (19) appears to guarantee that the total transmitted power and the total received power of the MIMO channel are the same with that of a single-input single-output (SISO) channel. To evaluate the AAR, it is required to characterize the statistic of the combined signal. Specifically in this case, we need to deal with the distribution of the sum of $MN$ correlated G-G RVs $I = \sum_{n=1}^{N} \sum_{m=1}^{M} I_{mn}$. According to *Proposition 1*, $I$ can be approximated by a G-G RV $\tilde{I}$ whose PDF is given by

$$f_{\tilde{I}}(\tilde{i}) = \frac{2\left(\frac{\overline{\alpha}_s \overline{\beta}_s}{MN}\right)^{\frac{\overline{\alpha}_s+\overline{\beta}_s}{2}}}{\Gamma(\overline{\alpha}_s)\Gamma(\overline{\beta}_s)} \tilde{i}^{\frac{\overline{\alpha}_s+\overline{\beta}_s}{2}-1} K_{\overline{\alpha}_s-\overline{\beta}_s}\left(2\sqrt{\frac{\overline{\alpha}_s\overline{\beta}_s}{MN}\tilde{i}}\right), \tag{20}$$

where $\overline{\alpha}_s$ and $\overline{\beta}_s$ are the shaping parameters of $\tilde{I}$, whose values are obtained by *Proposition 1*.

From Eq. (19), as $P$ is normalized to unity, the instantaneous SNR $\gamma$ is given by $\gamma = \frac{(\eta I)^2}{M^2N^2N_0} \approx \frac{(\eta \tilde{I})^2}{M^2N^2N_0}$ and after some simple mathematical transformations, we obtain the PDF of $\gamma$ as

$$f_\gamma(\gamma) = \frac{\left(\frac{\overline{\alpha}_s\overline{\beta}_s}{MN}\right)^{\frac{\overline{\alpha}_s+\overline{\beta}_s}{2}}}{\Gamma(\overline{\alpha}_s)\Gamma(\overline{\beta}_s)} \frac{\gamma^{\frac{\overline{\alpha}_s+\overline{\beta}_s}{4}-1}}{\gamma_0^{\frac{\overline{\alpha}_s+\overline{\beta}_s}{4}}} K_{\overline{\alpha}_s-\overline{\beta}_s}\left(2\sqrt{\frac{\overline{\alpha}_s\overline{\beta}_s}{MN}\sqrt{\frac{\gamma}{\gamma_0}}}\right), \tag{21}$$

where $\gamma_0 = \frac{\eta^2}{M^2N^2N_0}$. Plugging Eq. (21) into Eq. (18), then expressing the logarithmic and the Bessel functions in terms of the Meijer-G functions [40, Eq. (8.4.6.5)] [40, Eq. (8.4.23.1)], a closed-form expression for the AAR can be obtained as

$$C = \frac{B}{4\pi} \frac{\left(\frac{\overline{\alpha}_s\overline{\beta}_s}{MN}\right)^{\frac{\overline{\alpha}_s+\overline{\beta}_s}{2}}}{\Gamma(\overline{\alpha}_s)\Gamma(\overline{\beta}_s)} \frac{1}{\gamma_0^{\frac{\overline{\alpha}_s+\overline{\beta}_s}{4}}} \times G_{2,6}^{6,1}\left[\frac{\overline{\alpha}_s{}^2\overline{\beta}_s{}^2}{16M^2N^2\gamma_0}\middle| \begin{matrix} -\frac{\overline{\alpha}_s+\overline{\beta}_s}{4}, -\frac{\overline{\alpha}_s+\overline{\beta}_s}{4}+1 \\ \frac{\overline{\alpha}_s-\overline{\beta}_s}{4}, \frac{\overline{\alpha}_s+\overline{\beta}_s+2}{4} \\ \frac{\overline{\beta}_s-\overline{\alpha}_s}{4}, \frac{\overline{\beta}_s-\overline{\alpha}_s+2}{4}, -\frac{\overline{\alpha}_s+\overline{\beta}_s}{4}, -\frac{\overline{\alpha}_s+\overline{\beta}_s}{4} \end{matrix}\right]. \tag{22}$$

*2) Maximum Ratio Combining (MRC):* In the case of MRC scheme, the gain of each sub-channel is made proportional to the received signal intensity. The total transmitted power is also normalized to unity, resulting in the combined signal

$$r = \frac{x\eta}{M\sqrt{N}} \sqrt{\sum_{n=1}^{N} I_n^2} + z, \tag{23}$$

where $I_n = \sum_{m=1}^{M} I_{mn}$ is the combined signal at the $n-$th receiver. Compared to the case of EGC, in this combining scheme, the combined signal involves the square of the sum of G-G RVs which is more cumbersome to handle. To calculate the AAR in this case, we utilize the moment generating function (MGF)-based framework developed in [26]. According to this method, Eq. (18) can be expressed in the following form

$$C = \frac{1}{\ln 2} \int_0^\infty E_i(-\gamma) \mathcal{M}_\gamma^{(1)}(\gamma) \mathrm{d}\gamma, \tag{24}$$

where $E_i(\cdot)$ is the exponential integral function [41, Eq. (5.1.2)] and $\mathcal{M}_\gamma^{(1)}(\gamma)$ is the first derivative of the MGF of $\gamma$. Using [26, Corollary 2], Eq. (24) can be computed as

$$C = \frac{\pi}{Q \ln 2} \sum_{q=1}^{Q} \left[\frac{H\left(\frac{\tan(\theta_q)}{\sqrt{2}}\right)}{\sin(2\theta_q)}\right] + R_Q, \tag{25}$$

where $H(x) = xE_i(-x)\mathcal{M}_\gamma^{(1)}(x)$ and $\theta_q = (2q-1)\pi/(4Q)$. The remainder term $R_Q$ denotes the error as described in [41, Ch. 25]. From Eq. (23), the combined SNR is given by

$$\gamma = \frac{\eta^2}{M^2NN_0} \sum_{n=1}^{N} I_n^2 = \sum_{n=1}^{N} \gamma_n, \tag{26}$$

where $\gamma_n = \frac{\eta^2}{M^2NN_0} I_n^2$. As can be seen from Eq. (25), in order to compute the channel achievable rate, we first need to derive the MGF of $\gamma$. In the case of uncorrelated fading, $\mathcal{M}_\gamma(x)$

can be obtained as the product of the individual $\mathcal{M}_{\gamma_n}(x)$. However, in the case of correlated fading, it is necessary to find the joint probability distribution of $(\gamma_1, \gamma_2, \ldots, \gamma_N)$ for the derivation of $\mathcal{M}_{\gamma}(x)$.

To characterize the joint statistic of $(\gamma_1, \gamma_2, \ldots, \gamma_N)$, the distribution of $I_n$ should be known beforehand. Similar to the case of EGC, $I_n$ can be well approximated by a G-G RV $z_n \sim \Gamma\Gamma(\overline{\alpha}_n, \overline{\beta}_n, M)$ with its shaping parameters $\overline{\alpha}_n$, $\overline{\beta}_n$ are given by *Proposition 1*. Once $I_n$ is approximated as a G-G RV, $\gamma$ can be considered as a squared G-G RV. As a result, the PDF of $\gamma_n$ can be written as

$$f_{\gamma_n}(\gamma_n) = \frac{\left(\frac{\overline{\alpha}_n \overline{\beta}_n}{M}\right)^{\frac{\overline{\alpha}_n+\overline{\beta}_n}{2}}}{\Gamma(\overline{\alpha}_n)\Gamma(\overline{\beta}_n)} \frac{\gamma_n^{\frac{\overline{\alpha}_n+\overline{\beta}_n}{4}-1}}{\gamma_0^{\frac{\overline{\alpha}_n+\overline{\beta}_n}{4}}} \times K_{\overline{\alpha}_n-\overline{\beta}_n}\left(2\sqrt{\frac{\overline{\alpha}_n\overline{\beta}_n}{M}\sqrt{\frac{\gamma_n}{\gamma_0}}}\right), \quad (27)$$

where $\gamma_0 = \frac{\eta^2}{M^2 N N_0}$.

*Proposition 2:* The correlation coefficient $\varphi_{m,n}$ between $I_m$ and $I_n$ $(m \neq n)$ is given in Eq. (28) at the top of the next page, where $\rho_{mn,pq}$ denotes the correlation coefficient between the link connecting the $m-$th transmitter and the $n-$th receiver with that connecting the $p-$th transmitter and the $q-$th receiver.

*Proof:* See Appendix B.

Let us denote $\varphi_{l_{m,n}}$ and $\varphi_{s_{m,n}}$ be the large- and small-scale correlation coefficients between $I_m$ and $I_n$, respectively. Based on Eq. (12) with known $\varphi_{m,n}$ and the criteria for setting the correlation coefficients as stated in Section II, the values of $\varphi_{l_{m,n}}$ and $\varphi_{s_{m,n}}$ can easily be obtained. We then define $\mathbf{\Psi}_l$ and $\mathbf{\Psi}_s$ as the large- and small-scale correlation matrices, which are given by

$$\mathbf{\Psi}_l = \begin{pmatrix} \varphi_{l_{1,1}} & \varphi_{l_{1,2}} & \cdots & \varphi_{l_{1,N}} \\ \varphi_{l_{2,1}} & \varphi_{l_{2,2}} & \cdots & \varphi_{l_{2,N}} \\ \vdots & \vdots & \ddots & \vdots \\ \varphi_{l_{N,1}} & \varphi_{l_{N,2}} & \cdots & \varphi_{l_{N,N}} \end{pmatrix}, \quad (29)$$

$$\mathbf{\Psi}_s = \begin{pmatrix} \varphi_{s_{1,1}} & \varphi_{s_{1,2}} & \cdots & \varphi_{s_{1,N}} \\ \varphi_{s_{2,1}} & \varphi_{s_{2,2}} & \cdots & \varphi_{s_{2,N}} \\ \vdots & \vdots & \ddots & \vdots \\ \varphi_{s_{N,1}} & \varphi_{s_{N,2}} & \cdots & \varphi_{s_{N,N}} \end{pmatrix}, \quad (30)$$

respectively.

*Corollary 1:* The joint PDF of $N$ identically distributed squared G-G RVs $\gamma_1, \gamma_2, \cdots, \gamma_N$, i.e., $\overline{\alpha}_m = \overline{\alpha}_n = \overline{\alpha}$ and $\overline{\beta}_m = \overline{\beta}_n = \overline{\beta}$, is given by

$$f_{\boldsymbol{\gamma}}(\boldsymbol{\gamma}) = \frac{2^N |\mathbf{W}_l|^{\overline{\alpha}} |\mathbf{W}_s|^{\overline{\beta}}}{\Gamma(\overline{\alpha})\Gamma(\overline{\beta})} \sum_{\substack{i_1,\ldots,i_{N-1}=0 \\ k_1,\ldots,k_{N-1}=0}}^{\infty} \left(\frac{\overline{\alpha}\overline{\beta}}{M}\right)^{\frac{N(\overline{\alpha}+\overline{\beta})}{2}+\sum_{n=1}^{N-1}(i_n+k_n)} \times \prod_{n=1}^{N} \frac{\gamma_n^{\frac{\mu_n-1}{2}}}{\gamma_0^{\frac{\mu_n+1}{2}}} \frac{\omega_{s_{n,n}}}{\omega_{l_{n,n}}} K_{2\nu_n}\left(2\sqrt{\frac{\omega_{l_{n,n}}\omega_{s_{n,n}}\overline{\alpha}\overline{\beta}}{M}\sqrt{\frac{\gamma_n}{\gamma_0}}}\right) \times \prod_{n=1}^{N-1}\left[\frac{|\omega_{l_{n,n+1}}|^{2i_n}}{i_n!\Gamma(\overline{\alpha}+i_n)}\right]\left[\frac{|\omega_{s_{n,n+1}}|^{2k_n}}{k_n!\Gamma(\overline{\beta}+k_n)}\right], \quad (31)$$

where $\mu_n = \frac{\overline{\alpha}+\delta_j+\epsilon_n+\overline{\beta}}{2} - 1$, $\nu_n = \frac{\overline{\alpha}+\delta_n+\epsilon_n-\overline{\beta}}{2}$ with $\delta_n = i_n + k_j$, $\epsilon_n = i_n - k_n$ for $n = 1$, $\delta_n = i_{N-1} + k_{N-1}$, $\epsilon_n = i_{N-1} - k_{N-1}$ for $n = N$ and $\delta_n = i_{n-1} + i_n + k_{n-1} + k_n$, $\epsilon_n = i_{n-1} + i_n - k_{n-1} - k_n$ for $n = 2, 3, \ldots, N-1$. $\mathbf{W}_l$ and $\mathbf{W}_s$ denote the inverse of $\mathbf{\Psi}_l$ and $\mathbf{\Psi}_s$ with elements $\omega_{l_{m,n}}$ and $\omega_{s_{m,n}}$, respectively.

*Proof:* See Appendix C.

The joint PDF in (31) requires $\mathbf{W}_l$ and $\mathbf{W}_s$ to have the tridiagonal property. However, the inverses of $\mathbf{\Psi}_l$ and $\mathbf{\Psi_s}$ are not tridiagonal matrices in the general case. To make the expression in Eq. (31) applicable for arbitrary correlation matrices, one possible approach is to approximate $\mathbf{\Psi}_l$ and $\mathbf{\Psi_s}$ with Green matrices $\mathbf{C}_l$ and $\mathbf{C}_s$, respectively. Details on the Green maxtrix approximation can be found in [39].

*Corollary 2:* The joint MGF of $(\gamma_1, \gamma_2, \cdots, \gamma_N)$ is given by

$$\mathcal{M}_{\boldsymbol{\gamma}}(\boldsymbol{s}) = \frac{|\mathbf{W}_l|^{\overline{\alpha}} |\mathbf{W}_s|^{\overline{\beta}}}{\Gamma(\overline{\alpha})\Gamma(\overline{\beta})} \sum_{\substack{i_1,\ldots,i_{N-1}=0 \\ k_1,\ldots,k_{N-1}=0}}^{\infty} \left(\frac{\overline{\alpha}\overline{\beta}}{M}\right)^{\frac{N(\overline{\alpha}+\overline{\beta})}{2}+\sum_{n=1}^{N-1}(i_n+k_n)} \times \left(\frac{1}{4\pi}\right)^N \prod_{n=1}^{N} \frac{1}{\gamma_0^{\frac{\mu_n+1}{2}}} \left(\frac{\omega_{s_{n,n}}}{\omega_{l_{n,n}}}\right)^{\nu_n} s_n^{-\frac{\mu_n+1}{2}} \times G_{1,4}^{4,1}\left[\frac{(\omega_{s_{n,n}}\omega_{l_{n,n}}\overline{\alpha}\overline{\beta})^2}{16M^2\gamma_0 s_n}\middle| \begin{matrix} \frac{1-\mu_n}{2} \\ \frac{\nu_n}{2}, \frac{\nu_n+1}{2}, \frac{-\nu_n}{2}, \frac{-\nu_n+1}{2} \end{matrix}\right] \times \prod_{n=1}^{N-1}\left[\frac{|\omega_{l_{n,n+1}}|^{2i_n}}{i_n!\Gamma(\overline{\alpha}+i_n)}\right]\left[\frac{|\omega_{s_{n,n+1}}|^{2k_n}}{k_n!\Gamma(\overline{\beta}+k_n)}\right]. \quad (32)$$

*Proof:* Based on Eq. (31), the joint MGF of $(\gamma_1, \gamma_2, \cdots, \gamma_N)$ is given by

$$\mathcal{M}_{\boldsymbol{\gamma}}(\boldsymbol{s}) = \int_0^{\infty} \cdots \int_0^{\infty} \exp\left(-\sum_{n=1}^{N} s_n \gamma_n\right) f_{\boldsymbol{\gamma}}(\boldsymbol{\gamma}) \mathrm{d}\boldsymbol{\gamma}. \quad (33)$$

By expressing the Bessel function in terms of the Meijer-G function and using the identity [40, Eq. (2.24.1.1)], the joint MGF is derived as in Eq. (32) .

By denoting

$$A = \frac{|\mathbf{W}_l|^{\overline{\alpha}} |\mathbf{W}_s|^{\overline{\beta}}}{\Gamma(\overline{\alpha})\Gamma(\overline{\beta})} \sum_{\substack{i_1,\ldots,i_{N-1}=0 \\ k_1,\ldots,k_{N-1}=0}}^{\infty} \left(\frac{\overline{\alpha}\overline{\beta}}{M}\right)^{\frac{N(\overline{\alpha}+\overline{\beta})}{2}+\sum_{n=1}^{N-1}(i_n+k_n)} \times \left(\frac{1}{4\pi}\right)^N \prod_{n=1}^{N} \frac{1}{\gamma_0^{\frac{\mu_n+1}{2}}} \left(\frac{\omega_{s_{n,n}}}{\omega_{l_{n,n}}}\right)^{\nu_n} \times \prod_{n=1}^{N-1}\left[\frac{|\omega_{l_{n,n+1}}|^{2i_n}}{i_n!\Gamma(\overline{\alpha}+i_n)}\right]\left[\frac{|\omega_{s_{n,n+1}}|^{2k_n}}{k_n!\Gamma(\overline{\beta}+k_n)}\right], \quad (34)$$

and

$$B(s_n) = s_n^{-\frac{\mu_n+1}{2}} \times G_{1,4}^{4,1}\left[\frac{(\omega_{s_{n,n}}\omega_{l_{n,n}}\overline{\alpha}\overline{\beta})^2}{16M^2\gamma_0 s_n}\middle| \begin{matrix} \frac{1-\mu_n}{2} \\ \frac{\nu_n}{2}, \frac{\nu_n+1}{2}, \frac{-\nu_n}{2}, \frac{-\nu_n+1}{2} \end{matrix}\right], \quad (35)$$

$$\varphi_{m,n} = \frac{\sum_{i=1}^{M}\sum_{j=1}^{M}\rho_{mi,nj}}{\sqrt{\left(M+2\sum_{i=1}^{M}\sum_{j=i+1}^{M}\rho_{mi,mj}\right)\left(M+2\sum_{i=1}^{M}\sum_{j=i+1}^{M}\rho_{ni,nj}\right)}} \tag{28}$$

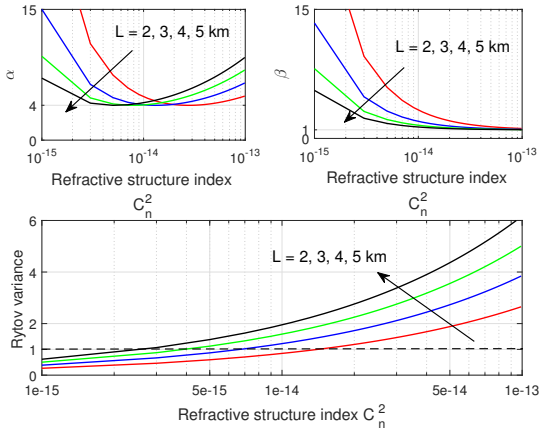


Figure 6: Effective numbers of large-, small-scale turbulences and Rytov variance versus the refractive structure index for different transmission distances.

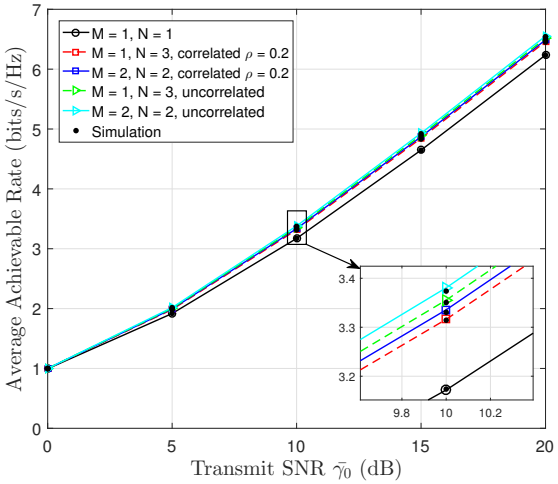


Figure 7: AAR versus transmit SNR for different number of transmitters and receivers with EGC scheme, $C_n^2 = 5\times10^{-15}$.

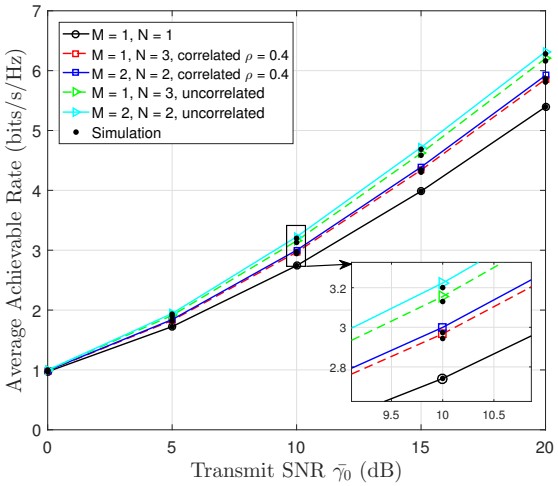


Figure 8: AAR versus transmit SNR for different number of transmitters and receivers with EGC scheme, $C_n^2 = 5\times10^{-14}$.

Eq. (32) can be rewritten as

$$\mathcal{M}_{\boldsymbol{\gamma}}(\boldsymbol{s}) = A\prod_{n=1}^{N} B(s_n). \tag{36}$$

Taking the derivative with respect to $\boldsymbol{s}$, we obtain

$$\mathcal{M}^{(1)}_{\boldsymbol{\gamma}}(\boldsymbol{s}) = A\sum_{n=1}^{N}\left(B^{(1)}(s_n)\prod_{m=1,m\neq n}^{N} B(s_m)\right). \tag{37}$$

With the help of [40, Eq. (8.2.1.30)], the derivative of $B(s_j)$ can be given by

$$B^{(1)}(s_n) = -s_j^{-\frac{\mu_n+3}{2}} \times G_{2,5}^{4,2}\left[\frac{(\omega_{s_{n,n}}\omega_{l_{n,n}}\overline{\alpha}\overline{\beta})^2}{16M^2\gamma_0 s_n}\middle| \begin{matrix} -\frac{\mu_n+1}{2}, \frac{1-\mu_n}{2} \\ \frac{\nu_n}{2}, \frac{\nu_n+1}{2}, \frac{-\nu_n}{2}, \frac{-\nu_n+1}{2}, \frac{1-\mu_n}{2}\end{matrix}\right]. \tag{38}$$

Finally, by substituting Eqs. (38) and (37) into Eq. (24), a closed-form expression for the AAR of the MRC scheme can be obtained.

## V. Numerical Results and Discussions

In this section, numerical results for the AAR derived in section IV are presented. Unless otherwise noted, the AWGN noise variance $N_0 = 2\times10^{-14}$ is assumed. The optical wavelength $\lambda = 1.55$ $\mu$m, the receiver aperture diameter $D = 8$ cm, the separation distance among apertures $d = 6$ cm and the link length $L = 2000$ m are chosen.

First, Fig. 6 illustrates the effective numbers of large-, small-scale turbulences and the Rytov variance $\sigma_R^2$ versus the refractive structure index $C_n^2$ for different transmission distances. Typically, weak, moderate and strong turbulence conditions correspond to $\sigma_R^2 < 1$, $\sigma_R^2 \approx 1$ and $\sigma_R^2 > 1$, respectively. As mentioned previously in the paper, we are interested in weak and strong turbulence regimes whose representative $C_n^2$ values at a 2 km transmission link are chosen to be $5\times10^{-15}$ and $5\times10^{-14}$, respectively. For the examined transmission distances, we observed that the value of $\alpha$ is always approximately greater than 4. The value of $\beta$ is inversely proportional to $C_n^2$ and approaches 1 as $C_n^2$ goes

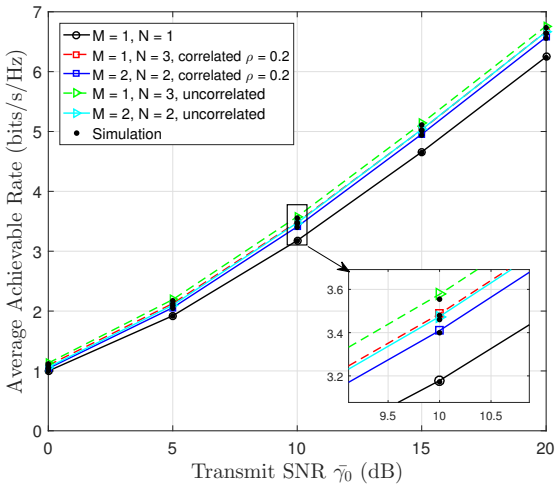


Figure 9: AAR versus transmit SNR for different number of transmitters and receivers with MRC scheme, $C_n^2 = 5\times10^{-15}$.

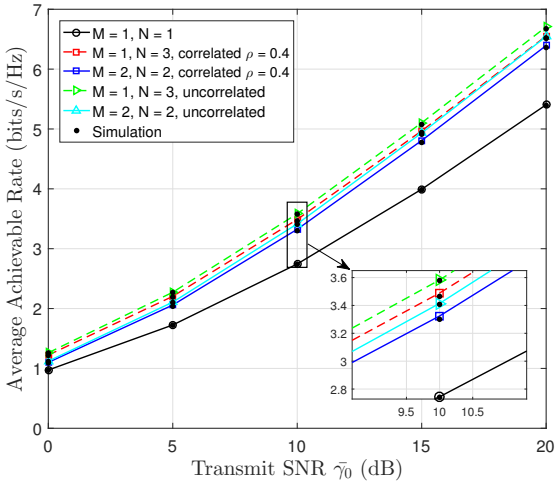


Figure 10: AAR versus transmit SNR for different number of transmitters and receivers with MRC scheme, $C_n^2 = 5\times10^{-14}$.

to infinity. According to the KS test results in Figs. 4 and 5, since there is at least one effective number parameter larger than 4, the approximation method in Section II is valid to use.

Figures 7 and 8 show the AAR of the EGC scheme versus the transmit SNR $\bar{\gamma}_0 = \frac{\eta^2}{N_0}$ with different numbers of transmitters and receivers for weak and strong turbulence conditions. Both uncorrelated and correlated fading cases are taken into considered. In the case of correlated fading, the correlation coefficients are $\rho = 0.2$ and $0.4$ for weak and strong turbulence, respectively. These values of the correlation coefficient are obtained through Fig. 1a under the aforementioned system parameters. M-C simulations are performed and a good agreement between the analytical and the simulation results can be confirmed. In the case of weak turbulence, it is obvious that the impact of channel correlation is negligible, i.e., the gap between uncorrelated and correlated performance is small due to the small value of the correlation coefficient. In the case of strong turbulence, however, the effect of channel correlation is more severe as we observed a clear performance degradation in the case of correlated channel. Also, it is seen that deploying diversity at both transmitter and receiver, i.e., $2 \times 2$ MIMO configuration, results in a slightly better performance compared to having receive diversity only, i.e., $1 \times 3$ MIMO configuration. Furthermore, the two figures confirm the benefit of using MIMO transmission, especially in strong turbulence conditions. At the rate of $4$ bits/s/Hz, the uncorrelated and correlated $2 \times 2$ MIMO systems achieve $2.4$ dB and $1.4$ dB power gains, respectively, for the strong turbulence regime. In the case of weak turbulence, these gains are $0.8$ dB and $0.6$ dB, respectively. The accuracy of the Green matrix approximation is confirmed in the case of correlated $1 \times 3$ MIMO. Assume that the apertures are placed circularly so that their separations are the same, the small- and large-scale correlation matrices are identical and given by

$$\mathbf{\Psi} = \begin{pmatrix} 1 & 0.2116 & 0.2116 \\ 0.2116 & 1 & 0.2116 \\ 0.2116 & 0.2116 & 1 \end{pmatrix}, \tag{39}$$

whose inverse is not tridiagonal. A Green matrix approximation to $\mathbf{\Psi}$ is obtained as

$$\mathbf{C} = \begin{pmatrix} 1 & 0.25 & 0.0625 \\ 0.25 & 1 & 0.25 \\ 0.0625 & 0.25 & 1 \end{pmatrix}, \tag{40}$$

with the mean square error of 0.0056.

In Figs. 9 and 10, the AAR of the MRC scheme with the same setting as in the EGC case is depicted for weak and strong turbulence regimes. First, it is confirmed that the MRC scheme outperforms the EGC one in both uncorrelated and correlated scenarios. Interestingly, unlike the EGC scheme, the $1\times3$ configuration performs better than the $2\times2$ configuration. Thus, the higher diversity order (i.e., the number of sub-channels) means the greater diversity gain. In case of MRC, as the output SNR is the sum of SNRs at each receive aperture, hence the more receiver apertures generally offers better performance (e.g., the $1 \times 3$ SIMO with 3 receive apertures performs better than the $2 \times 2$ MIMO with 2 receive apertures does). However, one must take the number of transmitters (in MIMO configurations) into account as well. If the number of transmitters is large, the combined signal quality at each receive aperture in MIMO configurations is much better than that in SIMO ones. In this case, the results in these figures may not hold. For the EGC scheme in strong turbulence condition and at the capacity of $4$ bits/s/Hz, the correlated $2 \times 2$ and $1 \times 3$ MIMO systems result in $1.2$ dB and $0.9$ dB power penalties compared to the uncorrelated ones. In the case of MRC, these power penalties are both $0.4$ dB. This reveals that the MRC scheme is more resilient to the channel correlation than the EGC is. For the correlated $1\times3$ MIMO in this strong turbulence scenario, the large-scale correlation matrix is given by

$$\mathbf{\Psi}_l = \begin{pmatrix} 1 & 0.6225 & 0.6225 \\ 0.6225 & 1 & 0.6225 \\ 0.6225 & 0.6225 & 1 \end{pmatrix}, \tag{41}$$

whose approximating Green matrix is

$$\mathbf{C}_l = \begin{pmatrix} 1 & 0.7059 & 0.5 \\ 0.7059 & 1 & 0.7083 \\ 0.5 & 0.7083 & 1 \end{pmatrix}, \tag{42}$$

where the mean square error is 0.0065.

## VI. Conclusions

This paper studied the AAR of spatial dviersity MIMO-FSO systems over correlated G-G fading channels. The closed-form expressions for the both schemes of EGC and MRC were analytically derived by employing the Green matrix approximation and a novel method to the sum of correlated G-G RVs. Numerical results and M-C simulations confirmed the validity of these approximations. It was seen that in the case of weak turbulence, the channel correlation was relatively small. Its impact on the AAR was thus negligible. When the turbulence became stronger, the channel correlation considerably degraded the capacity performance and the use of MIMO transmission proved to be essential to alleviate this negative effect.

## Acknowledgments

This work was supported by the Telecommunication Advancement Foundation (TAF) of Japan and the Vietnam National Foundation for Science and Technology Development (NAFOSTED) under grant number 102.02-2015.06.

## Appendix A
## Proof of Proposition 1

Suppose that the sum of $K$ identically but not necessarily independently distributed G-G RVs $X_i \sim \Gamma\Gamma(\alpha, \beta, \Omega)$ $(i = 1, \cdots, K)$ is approximated by a G-G RV $Y \sim \Gamma\Gamma(\overline{\alpha}_s, \overline{\beta}_s, \overline{\Omega}_s)$, i.e., $Y \approx \sum_{i=1}^{K} X_i$. The first and second moments of $\sum_{i=1}^{K} X_i$ are given by

$$\mathbb{E}\Big[\sum_{i=1}^{K} X_i\Big] = \sum_{i=1}^{K} \mathbb{E}[X_i] = K\Omega, \tag{43}$$

and

$$\begin{aligned}
&\mathbb{E}\left[\left(\sum_{i=1}^{K} X_i\right)^2\right] = \sum_{i=1}^{K} \mathbb{E}\left[X_i^2\right] + 2\sum_{i=1}^{K}\sum_{j=i+1}^{K} \mathbb{E}\left[X_i X_j\right] \\
&= \sum_{i=1}^{K} \mathbb{E}\left[X_i^2\right] + 2\sum_{i=1}^{K}\sum_{j=i+1}^{K} \Big(\mathbb{E}[X_i]\mathbb{E}[X_j] \\
&+ \rho_{ij}\sqrt{\mathrm{Var}(X_i)\mathrm{Var}(X_j)}\Big) \\
&= \sum_{i=1}^{K} \mathbb{E}\left[X_i^2\right] + 2\sum_{i=1}^{K}\sum_{j=i+1}^{K} \left(\Omega^2 + \rho_{ij}\sigma^2\right).
\end{aligned} \tag{44}$$

The variance of $\sum_{i=1}^{K} X_i$ is then given by

$$\begin{aligned}
\mathrm{Var}(Y) &= \mathbb{E}\left[\left(\sum_{i=1}^{K} X_i\right)^2\right] - \left(\mathbb{E}\left[\sum_{i=1}^{M} X_i\right]\right)^2 \\
&= \sum_{i=1}^{K} \mathrm{Var}\left(X_i\right) + 2\sum_{i=1}^{K}\sum_{j=i+1}^{K} \rho_{ij}\sigma^2 \\
&= \left(\frac{1}{\alpha} + \frac{1}{\beta} + \frac{1}{\alpha\beta}\right)\left(K + 2\sum_{i=1}^{K}\sum_{j=i+1}^{K} \rho_{ij}\right)\Omega^2.
\end{aligned} \tag{45}$$

On the other hand, the mean and variance of $Y$ are written as

$$\mathbb{E}[Y] = \Omega_s, \tag{46}$$

and

$$\mathrm{Var}(Y) = \left(\frac{1}{\overline{\alpha}_s} + \frac{1}{\overline{\beta}_s} + \frac{1}{\overline{\alpha}_s\overline{\beta}_s}\right)\overline{\Omega}_s^2 \tag{47}$$

Matching the mean and variance of $Y$ with that of $\sum_{i=1}^{K} X_i$ yields $\overline{\Omega}_s = K\Omega$, and

$$\begin{aligned}
&K^2\left(\frac{1}{\overline{\alpha}_s} + \frac{1}{\overline{\beta}_s} + \frac{1}{\overline{\alpha}_s\overline{\beta}_s}\right) \\
&= \left(\frac{1}{\alpha} + \frac{1}{\beta} + \frac{1}{\alpha\beta}\right)\left(K + 2\sum_{i=1}^{K}\sum_{j=i+1}^{K} \rho_{ij}\right).
\end{aligned} \tag{48}$$

To solve $\overline{\alpha}_s$ and $\overline{\beta}_s$, it is required to have one more equation which can be obtained from matching higher moments. However, it will lead to complex expressions. For simplicity, an approximate solution to Eq. (48) can be given by

$$\overline{\alpha}_s = K\left(1 + \frac{2}{K}\sum_{i=1}^{K}\sum_{j=i+1}^{K} \rho_{ij}\right)^{-1}\alpha, \tag{49}$$

$$\overline{\beta}_s = K\left(1 + \frac{2}{K}\sum_{i=1}^{K}\sum_{j=i+1}^{K} \rho_{ij}\right)^{-1}\beta, \tag{50}$$

This also completes the proof.

## Appendix B
## Proof of Proposition 2

The correlation coefficient between $I_m$ and $I_n$ is given by

$$\varphi_{mn} = \frac{\mathbb{E}[I_m I_n] - \mathbb{E}[I_m]\mathbb{E}[I_n]}{\sqrt{\mathrm{Var}(I_m)\mathrm{Var}(I_n)}}. \tag{51}$$

Firstly, the numerator can be written as

$$\begin{aligned}\mathbb{E}[I_m I_n] - \mathbb{E}[I_m]\mathbb{E}[I_n] &= \mathbb{E}\left[\left(\sum_{i=1}^{M} I_{mi}\right)\left(\sum_{j=1}^{M} I_{nj}\right)\right] \\ &- \mathbb{E}\left[\sum_{i=1}^{M} I_{mi}\right]\mathbb{E}\left[\sum_{j=1}^{M} I_{nj}\right] \\ &= \sum_{i=1}^{M}\sum_{j=1}^{M}\mathbb{E}\left[I_{mi}I_{nj}\right] - \sum_{i=1}^{M}\sum_{j=1}^{M}\mathbb{E}\left[I_{mi}\right]\mathbb{E}\left[I_{nj}\right] \\ &= \sum_{i=1}^{M}\sum_{j=1}^{M}\left(\rho_{mi,nj}\sqrt{\mathrm{Var}(I_{mi})\mathrm{Var}(I_{nj})}\right) \\ &= \sum_{i=1}^{M}\sum_{j=1}^{M}\left(\rho_{mi,nj}\sigma^2\right), \end{aligned} \tag{52}$$

where $\sigma^2$ is the variance of $I_{mi}$ and $I_{nj}$.

Next, for the denominator in Eq. (51)

$$\begin{aligned}\mathrm{Var}(I_m) &= \mathbb{E}[I_m^2] - \left(\mathbb{E}[I_m]\right)^2 \\ &= \mathbb{E}\left[\left(\sum_{i=1}^{M} I_{mi}\right)^2\right] - \left(\sum_{i=1}^{M}\mathbb{E}[I_{mi}]\right)^2 \\ &= \sum_{i=1}^{M}\left(\mathbb{E}[I_{mi}^2] - \left(\mathbb{E}[I_{mi}]\right)^2\right) \\ &+ 2\sum_{i=1}^{M}\sum_{j=i+1}^{M}\left(\mathbb{E}[I_{mi}I_{mj}] - \mathbb{E}[I_{mi}]\mathbb{E}[I_{mj}]\right) \\ &= M\sigma^2 + 2\sum_{i=1}^{M}\sum_{j=i+1}^{M}\left(\rho_{mi,mj}\sigma^2\right). \end{aligned} \tag{53}$$

Similarly, we obtain

$$\mathrm{Var}(I_n) = M\sigma^2 + 2\sum_{i=1}^{M}\sum_{j=i+1}^{M}\left(\rho_{ni,nj}\sigma^2\right). \tag{54}$$

Substituting Eqs. (52), (53) and (54) into Eq. (51) we arrive at Eq. (28).

## Appendix C
## Proof of Corollary 1

It is well-known that a G-G RV can be derived from the product of two independent Gamma RVs [27]. Therefore, a multivariate squared G-G RVs can also be obtained from the product of two independent multivariate squared Gamma RVs. Assume that $\mathbf{r} \triangleq [r_1, r_2, \ldots, r_N]$ be a set of $N$ identically distributed Gamma RVs with the correlation matrix $\mathbf{\Psi}_l$ given in (29) and $\mathbb{E}[r_n] = M$ being the average power. The PDF of each element is written as

$$f_{r_n}(r_n) = \frac{\overline{\alpha}^{\overline{\alpha}}}{\Gamma(\overline{\alpha})M^{\overline{\alpha}}} r_n^{\overline{\alpha}-1} e^{-\frac{\overline{\alpha} r_n}{M}}, \tag{55}$$

where $\overline{\alpha}$ is the shape parameter.

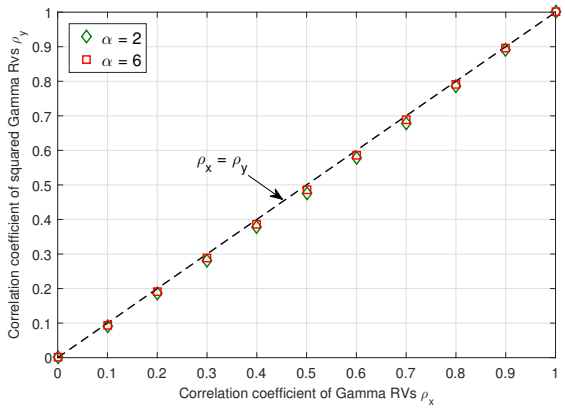


Figure 11: Correlation coefficients of Gamma and the corresponding squared Gamma RVs.

From [24, Eq. (5)], the joint PDF of $\mathbf{r}$ is expressed as

$$\begin{aligned} f_{\mathbf{r}}(\mathbf{r}) =& \frac{|\mathbf{W}_l|^{\overline{\alpha}} e^{-\sum_{n=1}^{N}\frac{\overline{\alpha}\omega_{l_{n,n}}}{M} r_n}}{\Gamma(\overline{\alpha})} \sum_{i_1,\ldots,i_{N-1}=0}^{\infty} r_1^{\overline{\alpha}+i_1-1} r_N^{\overline{\alpha}+i_{N-1}-1} \\ &\times \left(\frac{M}{\overline{\alpha}}\right)^{-N\overline{\alpha}-2\sum_{n=1}^{N-1} i_n} \prod_{n=2}^{N-1} r_n^{\overline{\alpha}+i_{n-1}+i_n-1} \\ &\times \prod_{n=1}^{N-1}\left[\frac{|\omega_{l_{n,n+1}}|^{2i_n}}{i_n!\Gamma(\overline{\alpha}+i_n)}\right]. \end{aligned} \tag{56}$$

To derive the joint PDF of a squared multivariate Gamma RV, its correlation matrix needs to be determined from the correlation matrix of the corresponding multivariate Gamma RV. To the best of authors' knowledge, there is no expression regarding the relationship between the two correlation matrices. However, the correlation coefficient of squared Gamma RVs can be taken identical to the corresponding coefficient of Gamma RVs with satisfactory accuracy as numerically validated in Fig. 11. Let $\mathbf{u} \triangleq [u_1, u_2, \ldots, u_N]$ be a set of $N$ squared Gamma RVs with $u_n = r_n^2$. After some simple mathematical manipulations, the joint PDF of $\mathbf{u}$ can be written as

$$\begin{aligned} f_{\mathbf{u}}(\mathbf{u}) =& \frac{|\mathbf{W}_l|^{\overline{\alpha}} e^{-\sum_{n=1}^{N}\frac{\overline{\alpha}\omega_{l_{n,n}}}{M} u_n^{\frac{1}{2}}}}{2^N\Gamma(\overline{\alpha})} \\ &\times \sum_{i_1,\ldots,i_{N-1}=0}^{\infty} u_1^{\frac{1}{2}(\overline{\alpha}+i_1)-1} u_N^{\frac{1}{2}(\overline{\alpha}+i_{N-1})-1} \\ &\times \left(\frac{M}{\overline{\alpha}}\right)^{-N\overline{\alpha}-2\sum_{n=1}^{N-1} i_n} \prod_{n=2}^{N-1} u_n^{\frac{1}{2}(\overline{\alpha}+i_{n-1}+i_n)-1} \\ &\times \prod_{n=1}^{N-1}\left[\frac{|\omega_{l_{n,n+1}}|^{2i_n}}{i_n!\Gamma(\overline{\alpha}+i_n)}\right]. \end{aligned} \tag{57}$$

Next, let $\mathbf{t} \triangleq [t_1, t_2, \ldots, t_N]$ be a set of $N$ identically distributed Gamma RVs with the correlation matrix $\mathbf{W}_s$, shape parameter $\overline{\beta}$ and assume that $\mathbb{E}[t_n] = 1$. Similarly, let $\mathbf{v} \triangleq [v_1, v_2, \ldots, v_N]$ be a set squared Gamma RVs with

$v_n = t_n^2$, the joint PDF of $\mathbf{v}$ can be expressed as

$$f_{\mathbf{v}}(\mathbf{v}) = \frac{|\mathbf{W}_s|^{\overline{\beta}} e^{-\sum_{n=1}^{N} \overline{\beta}\omega_{s_{n,n}} v_n^{\frac{1}{2}}}}{2^N \Gamma(\overline{\beta})} \times \sum_{i_1,\ldots,i_{N-1}=0}^{\infty} v_1^{\frac{1}{2}(\overline{\beta}+i_1)-1} v_N^{\frac{1}{2}(\overline{\beta}+i_{N-1})-1} \times \left(\frac{1}{\overline{\beta}}\right)^{-N\overline{\beta}-2\sum_{n=1}^{N-1} i_n} \prod_{n=2}^{N-1} v_n^{\frac{1}{2}(\overline{\beta}+i_{n-1}+i_n)-1} \times \prod_{n=1}^{N-1} \left[\frac{|\omega_{s_{n,n+1}}|^{2i_n}}{i_n!\Gamma(\overline{\beta}+i_n)}\right]. \quad (58)$$

To obtain a multivariate squared G-G Rvs, let us define $\mathbf{z} \triangleq [z_1, z_2, \ldots, z_N]$ where $z_n = u_n v_n$. The joint PDF of $\mathbf{z}$ can be derived as

$$f_{\mathbf{z}}(\mathbf{z}) = \int_0^{\infty} \cdots \int_0^{\infty} \prod_{n=1}^{N} v_n^{-1} f_{\mathbf{u}}\left(\frac{\mathbf{z}}{\mathbf{v}}\right) f_{\mathbf{v}}(\mathbf{v}) \mathrm{d}\mathbf{v}. \quad (59)$$

By substituting (57) and (58) into (59) and with help of [42, Eq. (3.471.9)], the joint PDF of $\mathbf{z}$ is given by

$$f_{\mathbf{z}}(\mathbf{z}) = \frac{2^N |\mathbf{W}_l|^{\overline{\alpha}} |\mathbf{W}_s|^{\overline{\beta}}}{\Gamma(\overline{\alpha})\Gamma(\overline{\beta})} \sum_{\substack{i_1,\ldots,i_{N-1}=0 \\ k_1,\ldots,k_{N-1}=0}}^{\infty} \left(\frac{\overline{\alpha}\overline{\beta}}{M}\right)^{\frac{N(\overline{\alpha}+\overline{\beta})}{2} + \sum_{n=1}^{N-1}(i_n+k_n)} \times \prod_{n=1}^{N} z_n^{\frac{\mu_n-1}{2}} \frac{\omega_{s_{n,n}}}{\omega_{l_{n,n}}} K_{2\nu_n}\left(2\sqrt{\frac{\omega_{l_{n,n}}\omega_{s_{n,n}}\overline{\alpha}\overline{\beta}}{M}\sqrt{z_n}}\right) \times \prod_{n=1}^{N-1} \left[\frac{|\omega_{l_{n,n+1}}|^{2i_n}}{i_n!\Gamma(\overline{\alpha}+i_n)}\right]\left[\frac{|\omega_{s_{n,n+1}}|^{2k_n}}{k_n!\Gamma(\overline{\beta}+k_n)}\right]. \quad (60)$$

Finally, since $\gamma_n = \frac{\eta^2}{M^2 N N_0} z_n$, the joint PDF of $\boldsymbol{\gamma}$ is derived as in (31).

## REFERENCES


[1] H. Willebrand, B. S. Ghuman, "Free-space optics: enabling optical connectivity in today's networks," *Sams Publishing*, 2001.

[2] M. A. Khalighi, M. Uysal, "Survey on free space optical communication: A communication theory perspective," *IEEE Commun. Surveys Tuts.*, vol. 16, no. 4, pp. 2231–2258, Fourth quarter 2014.

[3] M. Safari, M. Uysal, "Relay-assisted free-space optical communication," *IEEE Trans. Wireless Commun.,* vol. 7, no. 12, pp. 5441–5449, Dec. 2008.

[4] M. Karimi, M. Nasiri-Kenari, "Free space optical communications via optical amplify-and-forward relaying," *J. Lightw. Techno.*, vol. 29, no. 2, pp. 242–248, Jan. 2011.

[5] S. Kazemlou, S. Hranilovic, S. Kumar, "All-optical multihop free-space optical communication systems," *J. Lightw. Techno.*, vol. 29, no. 18, pp. 2663–2669, Sept. 2011.

[6] A. A. Farid, S. Hranilovic, "Diversity gain and outage probability for MIMO free-space optical links with misalignment," *IEEE Trans. on Commun.,* vol. 60, no. 2, pp. 479–487, Feb. 2012.

[7] D. A. Luong, A. T. Pham, "Average capacity of MIMO free-space optical communications," in *Proc. of IEEE International Conference on Communications (ICC)*, pp. 3354–3358, 2014.

[8] J. Zhang, L. Dai, Y. Han, Y. Zhang, Z. Wang, "On the ergodic capacity of MIMO free-space optical systems over turbulence channels," *IEEE J. Sel. Areas Commun.,* vol. 33, no. 9, pp. 1925–1934, Sept. 2015.

[9] L. Zheng, D. N. C. Tse, "Diversity and multiplexing: a fundamental tradeoff in multiple-antenna channels," *IEEE Trans. Inf. Theory*, vol. 49, no. 5, pp. 1073–1096, May 2003.

[10] M. Uysal, J. Li, M. Yu, "Error rate performance analysis of coded free-space optical links over gamma-gamma atmospheric turbulence channels," *IEEE Trans. on Commun.*, vol. 5, no. 6, pp. 1229-1233, June 2006.

[11] E. Bayaki, R. Schober, R. K. Mallik, "Performance analysis of MIMO free-space optical systems in gamma-gamma fading," *IEEE Trans. on Commun.*, vol. 57, no. 11, pp. 3415–3424, Nov. 2009,

[12] P. Wang, L. Zhang, L. Guo, F. Huang, T. Shang, R. Wang, and Y. Yang, "Average BER of subcarrier intensity modulated free space optical systems over the exponentiated Weibull fading channels," *Opt. Express*, vol. 22, no. 17, pp. 20828–20841, Aug. 2014.

[13] M. M. Abadi, Z. Ghassemlooy, S. Zvanovec, M. R. Bhatnagar, M-A. Khalighi, and Y. Wu, "Impact of link parameters and channel correlation on the performance of FSO systems with the differential signaling technique," *IEEE J. Opt. Commun. Netw.*, vol. 9, no. 2, pp. 138–148, Feb. 2017.

[14] R. Priyadarshani, M. R. Bhatnagar, Z. Ghassemlooy, S. Zvanovec, "Effect of correlation on BER performance of the FSO-MISO system with repetition coding over Gamma-Gamma turbulence," *IEEE Photon. J.*, vol. 9, no. 5, Art. ID 7906215, Oct. 2017.

[15] ———————, "Outage analysis of a SIMO FSO system over an arbitrarily correlated $\mathcal{M}$-distributed channel," *IEEE Photon. Technol. Lett.*, vol. 30, no. 2, pp. 141–144, Jan. 2018.

[16] S. M. Navidpour, M. Uysal, and M. Kavehrad, "BER performance of free-space optical transmission with spatial diversity," *IEEE Trans. on Wireless Commun.*, vol. 6, no. 8, pp. 2813–2819, Aug. 2007.

[17] K. P. Peppas, G. C. Alexandropoulos, C. K. Datsikas, F. I. Lazarakis, "Multivariate gamma-gamma distribution with exponential correlation and its applications in radio frequency and optical wireless communications," *IET Microwaves Antennas Propag.,* vo. 5, no. 3, pp. 364–371, Feb. 2011.

[18] G. Yang, M. Khalighi, Z. Ghassemlooy, and S. Bourennane, "Performance evaluation of receive-diversity free-space optical communications over correlated gamma-gamma fading channels," *Appl. Opt.,* vol. 52, no. 24, pp. 5903–5911, Aug. 2013.

[19] J. A. Anguita, M. A. Neifeld, and B. V. Vasic, "Spatial correlation and irradiance statistics in a multiple-beam terrestrial free-space optical communication link," *Appl. Opt.,* vol. 46, pp. 6561–6571, Sept. 2007.

[20] Z. Chen, S. Yu, T. Wang, G. Wu, S. Wang, and W. Gu, "Channel correlation in aperture receiver diversity systems for free-space optical communication," *J. Opt.,* vol. 14, no. 12, p. 125710, Nov. 2012.

[21] S. M. Haas, J. H. Shapiro, "Capacity of wireless optical communications," *IEEE J. Sel. Areas Commun.,* vol. 21, no. 8, pp. 1346 –1357, Oct. 2003.

[22] K. Chakraborty, "Capacity of the MIMO optical fading channel," in *Proc. of IEEE International Symposium on Information Theory (ISIT)*, pp. 530–534, 2005.

[23] M. T. Dabiri, M. J. Saber, S. M. S. Sadough, "On the performance of multiplexing FSO MIMO links in log-normal fading with pointing errors," *IEEE J. Opt. Commun. Netw.*, vol.9, no. 11, pp. 974–983, Nov. 2017.

[24] J. Zhang, M. Matthaiou, G. Karagiannidis, L. Dai, "On the multivariate gamma-gamma ($\Gamma - \Gamma$) distribution with arbitrary correlation and applications in wireless communications," *IEEE Trans. Veh. Technol.,* vol. 65, no. 5, pp. 3834 – 3840, May 2016.

[25] Thanh V. Pham, Truong C. Thang, Anh T. Pham, "On the ergodic capacity of MIMO correlated gamma-gamma fading channels," in *Proc. of International Conference on Advanced Technologies for Communications (ATC)*, Oct. 2016.

[26] M. Di Renzo, F. Graziosi, F. Santucci, "Channel capacity over generalized fading channels: a novel MGF-based approach for performance analysis and design of wireless communication systems," *IEEE Trans. Veh. Technol.,* vol. 59, no.1, pp. 127–149, Jan. 2010.

[27] M. A. Al-Habash, R. L. Phillips, and L. C. Andrews, "Mathematical model for the irradiance probability density function of a laser beam propagating through turbulent media," *Opt. Eng.,* vol. 40, no. 8, pp. 1554–1562, 2001.

[28] L. C. Andrews and R. L. Phillips, "Laser beam propagation through random media," *2nd edition Bellingham, WA: SPIE*, 2005.

[29] P. S. Bithas, N.C. Sagias, P. T. Mathiopoulos, G. K. Karagiannidis, A. A. Rontogiannis, "On the performance analysis of digital communications over generalized-K fading channels," *IEEE Commun. Lett.* , vol. 10, no. 5, May 2006.

[30] G. Yang, M. Khalighi, S. Bourennane, and Z. Ghassemlooy, "Approximation to the sum of two correlated Gamma-Gamma variates and its applications in free-space optical communications," *IEEE Trans. Wireless Commun. Lett.*, vol. 1, no. 6, pp. 621–624, Sept. 2012.

[31] S. Al-Ahmadi, H. Yanikomeroglu, "On the statistics of the sum of correlated generalized-K RVs," in *Proc. of IEEE International Conference on Communications (ICC)*, pp. 1–5, 2010.

[32] G. Yang, M. Khalighi, Z. Ghassemlooy, and S. Bourennane, "Performance analysis of space-diversity free-space optical systems over the correlated Gamma-Gamma fading channel using Pade approximation method," *IET Commun.*, vol. 8, no. 13, pp. 2246–2255, Sept. 2014.

[33] W. W. Daniel, "Applied Nonparametric Statistics," *2nd edition PWS-Kent Publishing*, 1990.

[34] K. Zhang, Z. Song, Y. L. Guan, "Simulation of Nakagami fading channels with arbitrary cross-correlation and fading parameters," *IEEE Trans. Wireless Commun.*, vol. 3, no. 5, pp. 1463–1468, Sept. 2004.

[35] A. Papoulis, "Probability, random Variables, and stochastic processes," *3rd edition, McGraw-Hill*, 1991.

[36] E. J. Lee and V. W. S. Chan, "Part 1: optical communication over the clear turbulent atmospheric channel using diversity," *IEEE J. Sel. Areas Commun.*, vol. 22, no. 9, pp. 1896–1906, Nov. 2004.

[37] M. I. Petkovic, A. M. Cvetkovic, G. T. Djordjevic, and G. K. Karagiannidis, "Partial relay selection with outdated channel state estimation in mixed RF/FSO systems," *IEEE/OSA J. Lightw. Technol.*, vol. 33, no. 13, pp. 2860–2867, Mar. 2015.

[38] H. E. Nistazakis; E. A. Karagianni; A. D. Tsigopoulos; M. E. Fafalios; G. S. Tombras, "Average capacity of optical wireless communication systems over atmospheric turbulence channels," *J. Lightw. Technol.,* vol. 27, no. 8, pp. 974–979, Apr. 2009.

[39] G. K. Karagiannidis, D. A. Zogas, S. A. Kotsopoulos, "An efficient approach to multivariate Nakagami-m distribution using Green's matrix approximation," *IEEE Trans. on Wireless Commun.*, vol. 2, no. 5, pp. 883–889, Sept. 2003.

[40] A. P. Prudnikov, Y. A. Brychkov, and O. I. Marichev, "Integrals and Series. Vol. 3: More Special Functions," *Gordon and Breach Science Publishers*, 1990.

[41] M. Abramowitz, I. A. Stegun, "Handbook of mathematical functions with formulas, graphs, and mathematical tables," *New York: Dover*, 1972.

[42] I. S. Gradshteyn, I. M. Ryzhik, "Table of integrals series and products," *7th edition Academic Press*, 2007.